TECHNICAL REPORT

ISO/TR 21254-4

First edition
2011-09-01

Lasers and laser-related equipment — Test methods for laser-induced damage threshold —

Part 4:
Inspection, detection and measurement

Lasers et équipements associés aux lasers — Méthodes d'essai du seuil d'endommagement provoqué par laser —

Partie 4: Inspection, détection et mesurages

Reference number
ISO/TR 21254-4:2011(E)

Contents

Page

Foreword

ISO (the International Organization for Standardization) is a worldwide federation of national standards bodies (ISO member bodies). The work of preparing International Standards is normally carried out through ISO technical committees. Each member body interested in a subject for which a technical committee has been established has the right to be represented on that committee. International organizations, governmental and non-governmental, in liaison with ISO, also take part in the work. ISO collaborates closely with the International Electrotechnical Commission (IEC) on all matters of electrotechnical standardization.

International Standards are drafted in accordance with the rules given in the ISO/IEC Directives, Part 2.

The main task of technical committees is to prepare International Standards. Draft International Standards adopted by the technical committees are circulated to the member bodies for voting. Publication as an International Standard requires approval by at least 75 % of the member bodies casting a vote.

In exceptional circumstances, when a technical committee has collected data of a different kind from that which is normally published as an International Standard ("state of the art", for example), it may decide by a simple majority vote of its participating members to publish a Technical Report. A Technical Report is entirely informative in nature and does not have to be reviewed until the data it provides are considered to be no longer valid or useful.

Attention is drawn to the possibility that some of the elements of this document may be the subject of patent rights. ISO shall not be held responsible for identifying any or all such patent rights.

ISO/TR 21254-4 was prepared by Technical Committee ISO/TC 172, *Optics and photonics*, Subcommittee SC 9, *Electro-optical systems*.

ISO 21254 consists of the following parts, under the general title *Lasers and laser-related equipment — Test methods for laser-induced damage threshold*:

— *Part 1: Definition and general principles*

— *Part 2: Threshold determination*

— *Part 3: Assurance of laser power (energy) handling capabilities*

— *Part 4: Inspection, detection and measurement*

Introduction

Detection programmes for laser-induced damage threshold always involve sensitive techniques for the inspection of surfaces and the detection of damage. In a typical detection protocol, each sample is inspected prior to the test by microscopic methods to evaluate the surface quality and to assess imperfections. During the irradiation of the sample in S-on-1, damage testing, a variety of online-monitoring schemes is applied to detect damage.

Examples of these methods include the detection of light scattered by the test area, the collection of plasma radiation, or photothermal detection schemes. In most cases, the detection system is directly linked to the laser to interrupt the irradiation of the sample promptly at the first instance of damage. In this way catastrophic damage of the component can be avoided, and the number of pulses until the appearance of first damage can be determined precisely. Also, this direct information on the state of damage can be processed in the course of the running test to determine energy levels for the following interrogations optimised to minimise detection uncertainties. For the same reason, sophisticated detection schemes based on direct imaging and online image processing can be often found in 1-on-1 detection facilities. The irradiation sequence on the samples is followed by inspection using an appropriate technique to identify the damaged sites and to gain information on the contributing damage mechanisms. This inspection of the interrogated sites is essential for an accurate determination of the damage thresholds because it is the final and most sensitive assessment of the state of damage.

This Technical Report describes selected techniques for the inspection of optical surfaces prior to and after damage testing, and damage detection techniques integrated in detection facilities. The described damage detection methods are examples of practical solutions tested and often applied in detection facilities. The application of other schemes for the detection or inspection of damage in optical components is not excluded by this Technical Report.

Lasers and laser-related equipment — Test methods for laser-induced damage threshold —

Part 4: **Inspection, detection and measurement**

1 Scope

This part of ISO 21254 describes techniques for the inspection and detection of laser-induced damage on optical surfaces and in the bulk of optical components.

2 Normative references

The following referenced documents are indispensable for the application of this document. For dated references, only the edition cited applies. For undated references, the latest edition of the referenced document (including any amendments) applies.

ISO 11145, *Optics and photonics — Lasers and laser-related equipment — Vocabulary and symbols*

ISO 21254-1, *Lasers and laser-related equipment — Test methods for laser-induced damage threshold — Part 1: Definitions and general principles*

3 Terms and definitions

For the purposes of this document, the terms and definitions given in ISO 11145 and ISO 21254-1 apply.

4 Damage detection methods

4.1 General

For damage test methods involving more than one pulse per test site, an appropriate online damage detection system is needed to evaluate the state of the surface under test according ISO 21254-1. It is recommended that the online damage detection system should have the facility for cutting off subsequent pulses and for stopping the pulse counter after detection of damage.

For online damage detection, any appropriate principle can be used. Techniques suited to this purpose are for instance online microscopic techniques, photoacoustic and photothermal detection, as well as scatter detections using a separate laser or radiation from the damaging laser. In the following examples for online damage detection schemes are described which are based on the collection of radiation from the sample, the detection of specific sample properties, and photothermal methods. In addition, a technique based on transient pressure sensing is outlined as an example for a non-optical online detection method. The described techniques are illustrated by schemes published in the open literature. This selection of practical examples is considered for descriptive purposes only and does not indicate any preferences or recommendation for these schemes.

4.2 Summary of damage detection methods

The major features of the described online damage detection methods are compiled in Table 1. Besides the fundamental principle, specific advantages and disadvantages are considered.

Table 1 — Advantages and disadvantages of damage detection methods

Damage detection method (reference)	Advantages	Disadvantages
Scatter detection techniques (4.3.1)	▪ low experimental expense ▪ clear correlation to and preferred for morphological damage ▪ suitable for automatic sequences ▪ high sensitivity and reliability ▪ small reaction time (ns) ▪ selective detection of surface or bulk and surface damage	▪ indirect detection: signal not correlated to damage mechanism ▪ less suitable for layer structures with overcoatings or rugate filters ▪ not sensitive to compaction
Plasma and thermal radiation (4.3.2)	▪ low experimental expense ▪ signal amplitude correlated to damage mechanisms ▪ small reaction time (ns)	▪ dependent on environment ▪ reduced sensitivity: plasma radiation might appear without surface damage and vice versa ▪ signal interpretation with respect to damage difficult ▪ difficult data reduction
Fluorescence (4.3.3)	▪ signal correlated to damage mechanisms and interpretable ▪ small reaction time (ns) ▪ preferred for colour centre detection	▪ high experimental expense ▪ reduced sensitivity: correlation of damage to fluorescence signal might be complex and sample specific ▪ signal interpretation with respect to damage difficult ▪ material specific calibration necessary
Reflectance transmittance (4.4.1)	▪ low experimental expense ▪ high sensitivity and clear correlation to functional damage ▪ suitable for automatic sequences ▪ high reliability ▪ small reaction time (ns)	▪ indirect detection: signal not correlated to damage mechanism ▪ not suitable for all kind of optics
Online microscopy (4.4.2)	▪ direct image generation ▪ reliability best achievable for surfaces ▪ complex data reduction possible ▪ suitable for automatic sequences	▪ high experimental expense ▪ low response time (10 ms-range)
Photothermal deflection and lensing and Mirage effect (4.5)	▪ evaluation of absorptance ▪ high sensitivity ▪ signal correlated to damage mechanisms ▪ pre-damage effects detectable ▪ photoacoustic and thermal effects (Mirage effect)	▪ signal interpretation with respect to damage difficult ▪ low temporal resolution (ms)
Transient pressure sensing (4.6)	▪ vibration and misalignment insensitive ▪ suitable for curved or scattering samples ▪ analysis of ablated species possible allowing for an interpretation of damage mechanisms (with mass spectrometer)	▪ only suitable for high vacuum conditions ▪ not suitable for small (< 200 µm) spot sizes (low ablated mass)

4.3 Collection of radiation from the sample

4.3.1 Scatter detection techniques

A prominent concept for online damage detection is the collection of radiation scattered by the component under test. The increase in optical scattering of the test site is interpreted as a direct consequence of the bulk or surface properties altered by the contributing damage mechanisms. The arrangements can be operated directly by the detection of scattered radiation from the test laser (see Figure 1) or on the basis of scattering from a beam of a separate laser superimposed with the test laser beam on the test site (see Figure 2). In systems based on scattering of test laser radiation, the method can be implemented with a few additional optical components collecting the scattered radiation on a detector. For collection of the scattered radiation on the detector element lenses or concave mirrors are employed. For set-ups with separate source a laser with excellent pointing stability and minimum intensity fluctuations is used as radiation source. The laser light is refined by a beam preparation system that normally consists of telescope systems with apertures, spatial filters and optical components for modulating the laser power density. After beam preparation, the laser beam is focused onto the actual site of the specimen under damage test. The scattered radiation is collected by a lens and detected by a photo detector. The fraction of the laser beam reflected by the specimen surface is cut out by a negative aperture. To achieve high sensitivity and low interference with other light sources in the environment of the set-up, phase sensitive detection techniques and an interference filter for the laser wavelength are recommended. In all set-ups the detector signal should be recorded with sufficient temporal resolution to identify the onset of damage instantly in correlation to the individual pulses of the test laser.

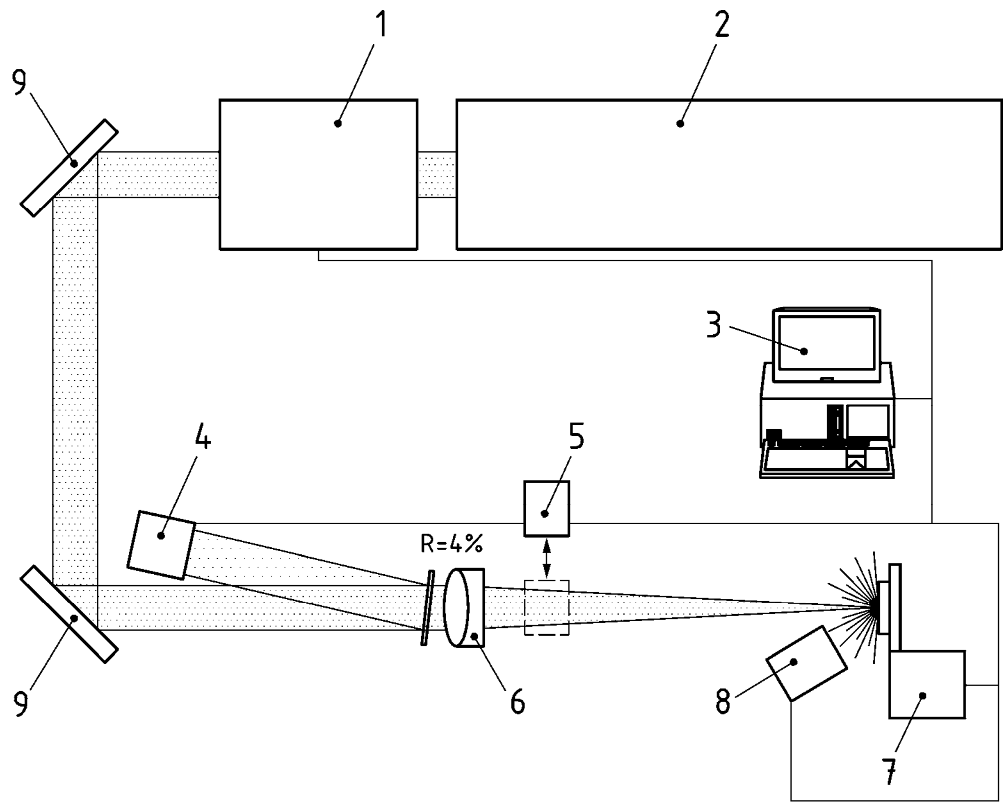

NOTE See Reference [5].

Key

1 motorized attenuator
2 Ti: Sapphire CPA-Laser
3 measurement controlling PC
4 energy detector
5 power meter
6 achromate
7 sample translator
8 online damage detector
9 HR 45°

Figure 1 — Typical set-up for an online scatter detection system on the basis of radiation scattered from the test laser beam

Scatter detection systems for damage detection demonstrate high reliability for damage mechanisms which influence the structure of the surface or induce defects in the bulk of the test sample. The detection scheme is occasionally not appropriate for specimens which are damaged by effects involving a complete delamination of coatings from the surface. In some cases a reduction of the scatter signal is observed during the initial irradiation phase which is attributed to surface cleaning or conditioning effects.

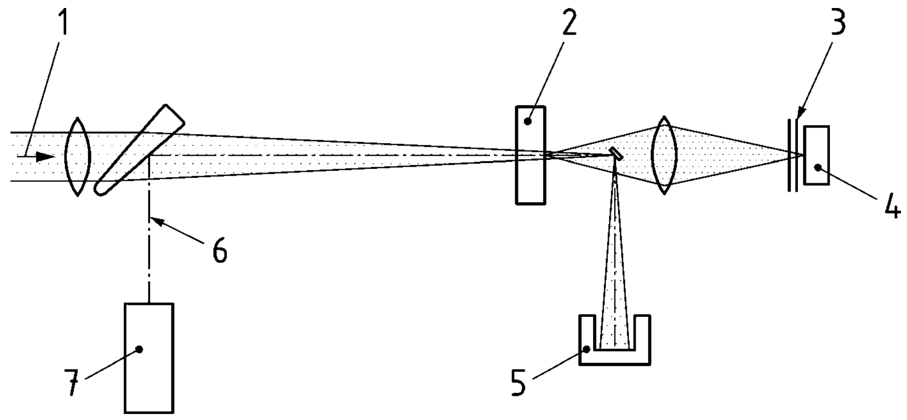

Key

1 test beam

2 test sample

3 filter stack

4 detector

5 beam dump

6 probe beam

7 probe laser

Figure 2 — Typical set-up for an online scatter detection system with a separate laser source and a negative aperture

4.3.2 Detection of plasma and thermal radiation

Often the emission of radiation from laser-induced plasma is observed in the event of surface damage[6][15]. This radiation can be detected as a damage indicator with an arrangement similar to the detection system used for direct online scatter detections. To select the plasma emission from the radiation of the test laser, a set of filters with high optical density for the test laser wavelength is recommended. Plasma radiation can be measured in a broad spectral range from the MIR to DUV. In some set-ups the wavelength is selected in the NIR and is simultaneously interpreted as a pyrometric signal for an in-situ detection of the sample temperature (see Figure 3). Although a temperature calibration of the system is dependent on a variety of specific parameters of the sample, the evaluation of the temperature radiation allows for additional insights into the contributing damage mechanisms. Detection schemes based on plasma radiation suffer from the fact that plasma can also occur during laser irradiation without surface damage.

4.3.3 Fluorescence

The spectrophotometric detection of fluorescence radiation allows for a detailed interpretation of electronic states and transitions during irradiation of the sample material. As a consequence of high photon energies the method offers interesting aspects for the damage testing in the UV/DUV-spectral range. In most cases, fluorescence occurs already at relatively small irradiation energies well below the damage threshold of the test component. Therefore, damage detection is dependent on a complex evaluation of the fluorescence spectra which restricts the principle to special applications and specimens.

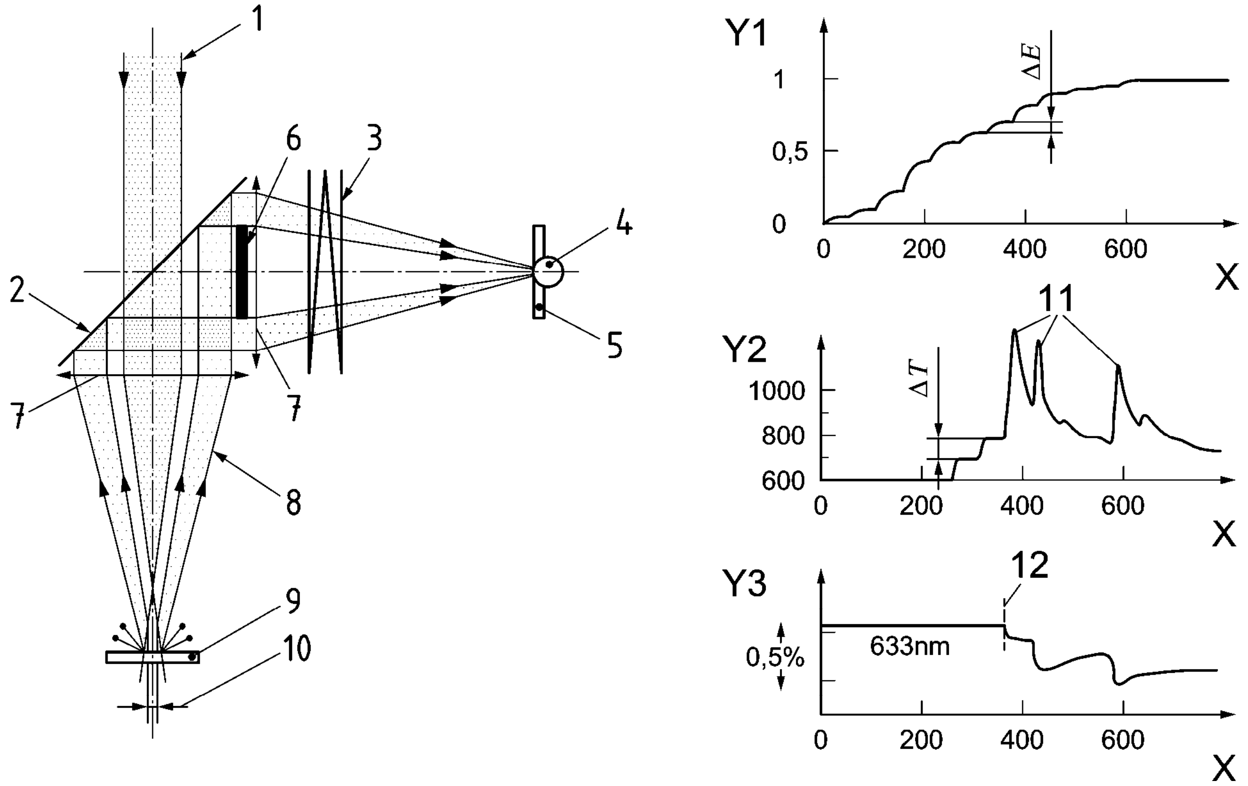

a) Example of a set-up

b) Signals detected during irradiation by a pulse train (12 pulses, λ = 1 064 nm, $d_{86,5}$ = 0,5 mm[6])

Key

1 incident laser beam
2 dichroitic beam splitter HT 1060/HR 850/45°
3 filter set HT 850/HR 1060
4 Si – photodiode
5 aperture adjusted for spot size
6 scatter field
7 focusing lens
8 temperature radiation
9 sample
10 spot size
11 plasma
12 damage
X time scale [µs]
Y1 energy [relative units]
Y2 temperature [°C]
Y3 transmission [%]

Figure 3 — Example of a set-up on the basis of radiation emitted by the sample surface during damage or laser heating; diagram depicting the signals detected during irradiation by a pulse train

4.4 Detection of changes in reflectance or transmittance and imaging techniques

4.4.1 Online detection of changes in reflectance or transmittance

During and after the event of damage, the optical transfer properties of specimen are significantly altered. This effect is the basis for a variety of damage detection schemes involving online detections of the changes in reflectance or transmittance of the specimen. Similar to the scatter detection schemes, the radiation of the test laser or of a separate source can be employed for the detection. Detection schemes for test laser radiation transmitted by the sample can be realized with a single detector unit which is placed behind the sample (see Figure 4). The detector unit contains attenuators to adjust the maximum laser power impinging onto the detector and an appropriate signal processing system with sufficient bandwidth to distinguish the effect of each individual pulse on the transmittance of the sample. The reliability of these systems is comparable to online scatter detection units. Samples with high transmittance or reflectance, as well as specimens with predominant bulk damage will require consideration with caution.

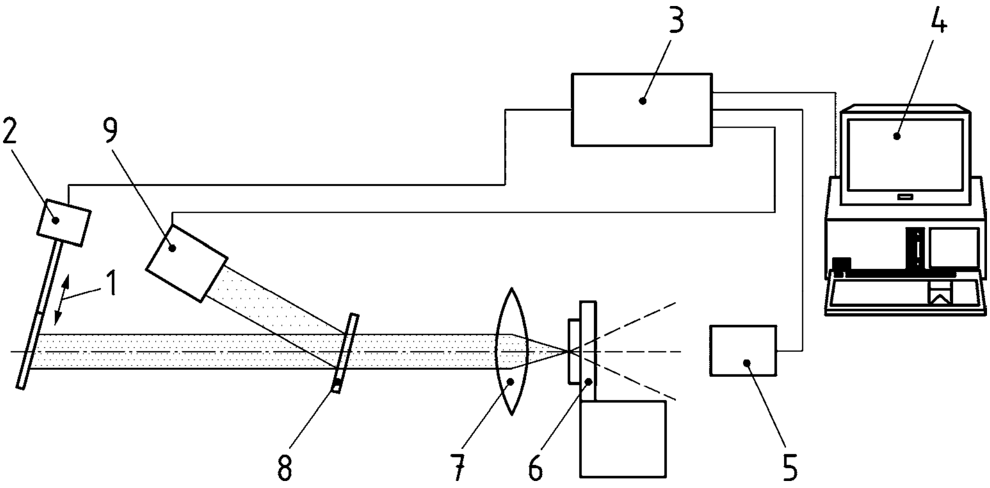

Key

1 HR
2 shutter
3 shutter control
4 controlling computer
5 detector
6 sample holder
7 focusing lens
8 PR 4 %
9 reference detector

NOTE See Reference [7].

Figure 4 — Example for a detection scheme based on a direct detection of transmittance at the test wavelength

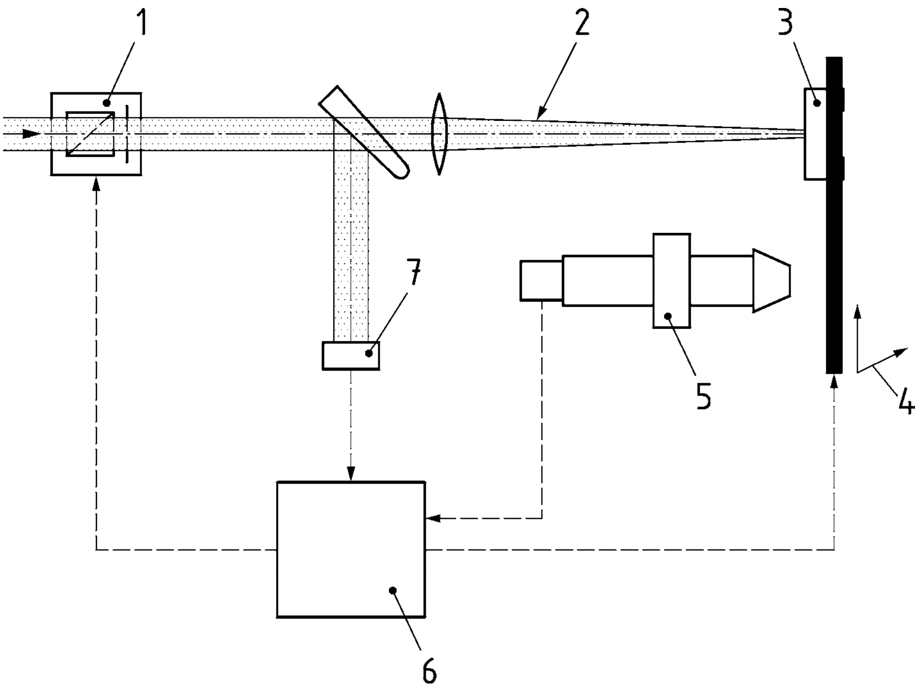

Key

1 attenuator
2 test beam
3 test sample
4 x/y motion stage
5 microscope and CCD camera
6 PC
7 energy detector

NOTE See Reference [8].

Figure 5 — Example for a set-up with a microscopic inspection system apart from the irradiation area

4.4.2 Online microscopy

Online microscopic systems allow for a direct inspection of the surface during the irradiation sequence. Often, in-situ microscopic systems are constructed using a long distance microscope which is linked to an electronic camera (see Figure 5). Images are processed in a computer typically with pixel by pixel comparing algorithms which define damage on the basis of a preselected number threshold of pixels altered by laser-induced damage (see Figure 6). As a consequence of the relatively time consuming data reduction process, the time resolution of online microscopic methods is restricted to the range of a few ten milliseconds. Also, the identification of a damage event is relatively complex and sensitive to influences from the environment. Laser cleaning effects are observed which might be interpreted as a damage event by online microscopic systems. Other limitations on the spatial resolution are imposed on the technique by the minimum pixel size of modern camera systems. In order to increase the resolution, a microscopic system with small working distance may be also mounted near the sample holder. In this configuration, the specimen can be translated from the irradiation area to the focus of the microscope by the sample stage. After inspection, the sample can be repositioned in the irradiation area. This technique is only practicable for 1-on-1 damage facilities or S-on-1 testing on the basis of the extrapolation method (see Figure 5).

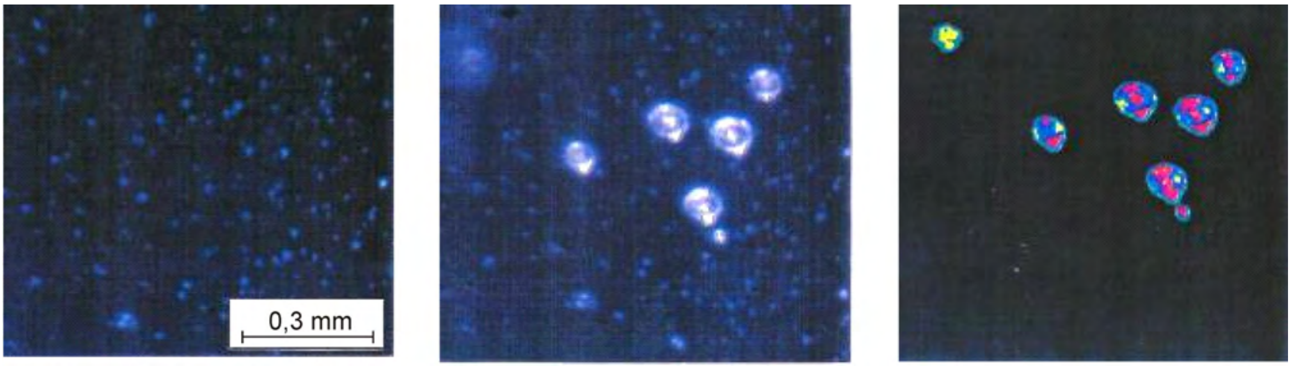

a) Example of the evaluation of microscopic images recorded before irradiation (TEA-CO_2-Laser) of sample surface

b) Example of the evaluation of microscopic images recorded after irradiation (TEA-CO_2-Laser) of sample surface

c) Damage sites are detected by an image comparator algorithm including false colour representation

NOTE See Reference [9].

Figure 6 — Images showing laser-induced damage

4.5 Photothermal detection schemes

4.5.1 General

A variety of different detection schemes can be employed to analyse the photothermal effects[16][17][18] occurring during damage. A general representation of these effects is given in Figure 7. Most of the schemes have been applied for damage detection. In the following, detection schemes will be considered which are more often employed. The interpretation of the monitored signals in respect to damage phenomena is extremely complex and cannot be performed without human intervention in most cases. Therefore, photothermal detection schemes are predominantly applied in fundamental research and are rarely found in damage detection facilities dedicated to routine quality control.

4.5.2 Photothermal deflection and surface thermal lensing

The principle of the photothermal deflection method is illustrated by detection scheme 2 (deflection technique) in Figure 7. As a consequence of the laser heating of the interrogated site, a bulge is formed which deflects the probe beam. For the detection of the photothermal deflection signal, a probe beam is directed onto the test site. The position of the reflected probe beam is monitored by a position sensitive detector. Surface displacements below 1 Å can be resolved. The major components of a surface thermal lensing experiment are depicted in Figure 8. In contrast to the thermal deflection effect, the deviation of the focus of the probe beam due to the laser-induced bulge is detected. Advantages of these two detection schemes are the relatively high sensitivity and the possibility to detect predamage phenomena. If the deflection system is calibrated to absorption, the dynamic behaviour of absorptance in the specimen can be also analysed.

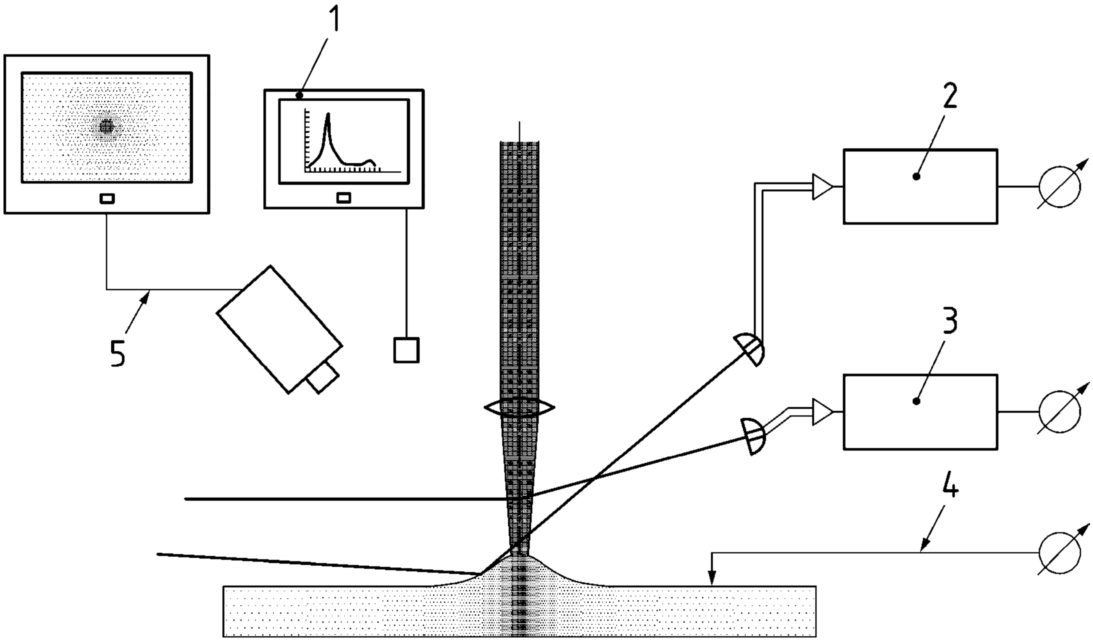

Key

1 photoacoustic technique
2 photothermal deformation or deflection technique
3 Mirage effect
4 laser calorimetry
5 radiometry

NOTE The different photothermal methods can be classified according to the detection channels for the laser-induced thermal effects. Examples are illustrated for photoacoustic techniques (1), photothermal deformation or deflection technique (2), the Mirage effect (3), laser calorimetry (4) and radiometry (5).

Figure 7 — Photothermal detection schemes

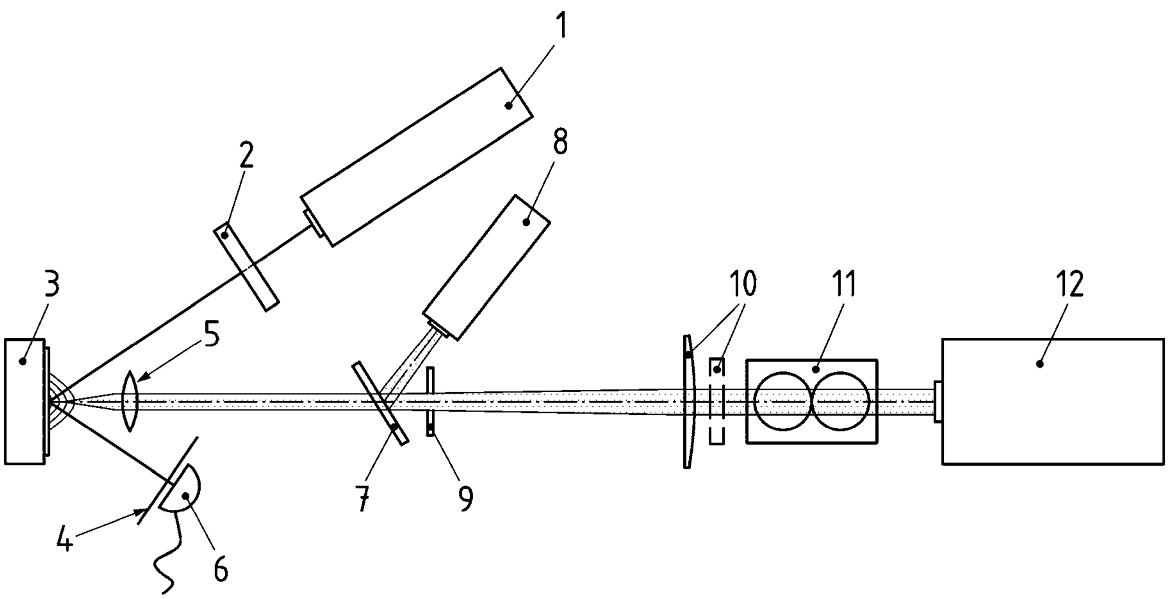

Key

1	HeNe-Laser	4	pinhole	7	beam splitter	10	homogenizer and field lens
2	attenuator	5	focusing lens	8	pyrometer	11	variable attenuator
3	sample	6	photodiode	9	mask	12	Eximer-Laser

NOTE See Reference [10].

Figure 8 — Example set-up for the detection of damage by surface thermal lensing

4.5.3 Mirage effect

The Mirage effect is based on the detection scheme 3 (Mirage effect) illustrated in Figure 7. As a consequence of the instantaneous heating of the surface, an acoustic shockwave (photoacoustic Mirage effect) is emitted and deflects the probe beam. Also heat is transported by heat conduction from the surface in the ambient material resulting in a transient change of the refractive index in the path of probe beam. This temperature wave also results in a deflection of the probe beam. The deflection of the probe beam is detected by a position sensitive detector or by an arrangement with a pinhole similar to the system depicted in Figure 8. The deflection signal of the photoacoustic Mirage effect (see Figure 9) may be also assessed in respect to different interaction mechanisms of the laser beam with the optical component.

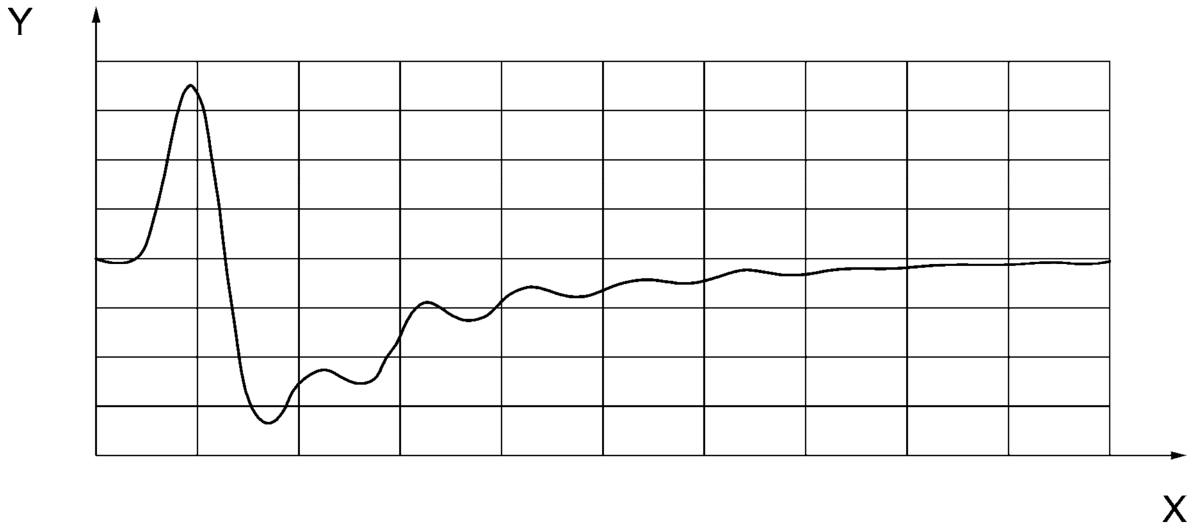

Key

X time scale [µs]

Y intensity P(t)

Figure 9 — Typical temporal variation of the probe beam deflection (photoacoustic Mirage effect, 0,25 µs/div) after damage of an optical component by a TEA-CO_2-Laser

4.6 Transient pressure sensing

In the case that optical components need to be tested under vacuum conditions an online damage monitoring method can be used that relies on a non-optical detection method. It is based on the detection of ablative components emitted from the irradiated surface concomitant with the occurrence of laser damage. The detection can be performed with cold cathode pressure sensors or generally with ionization gauges positioned in the neighbourhood of the sample under inspection. It has proven to operate very sensitively under high-vacuum conditions at a background pressure of < 10^{-4} mbar (at a pressure of 10^{-4} mbar, the molecular mean free path length is 0,5 m, which has to be compared with the size of the vacuum chamber). Ionization gauges sense the pressure indirectly by measuring the number of electrical ions produced when the gas is bombarded with electrons. Hence, neutral ablation products will be ionized, or emitted ions will be detected directly as a current from the cathode. As vacuum chambers are typically operated in a dynamic pumping mode, the pressure rise is of transient nature, i. e. the original pressure value will be recovered in less than 1 s after the damage incidence.

In Figure 10 a vacuum chamber is depicted with a pressure sensor mounted at a suitable distance from a sample under investigation. Particle or molecular emissions from the sample due to laser interaction will be collected by the sensor.

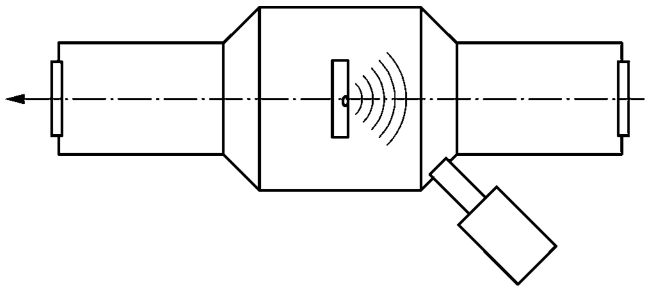

Figure 10 — Placement of a pressure sensor in the vicinity of the sample under test exposed to vacuum; ablated material is emitted and preferably detected in upstream direction

Transient pressure sensing can principally have a large kHz detection bandwidth, is insensitive to optical interference, and can be used to monitor damage incidences on curved surfaces or on strongly scattering samples like beam dumps. An example is shown in Figure 11, where the trace of a scatter detection is contrasted with a simultaneous pressure rise from a cold cathode sensor placed 200 mm apart from the sample. For investigations in the ablated species, a residual gas analyser may be also attached to the vacuum chamber.

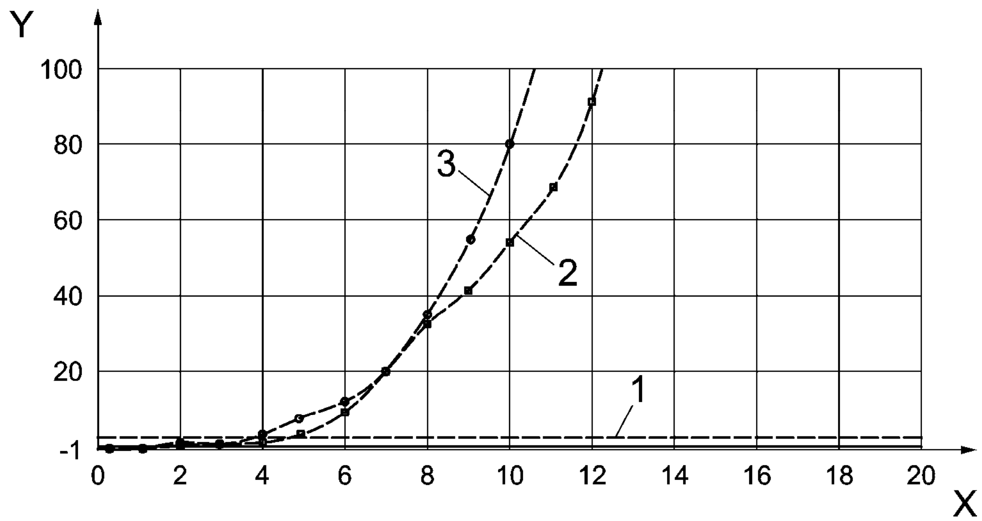

Key

X pulse number

Y amplitude [a.u]

1 threshold

2 scatter

3 pressure

Figure 11 — Scatter trace and pressure trace due to damage which has occurred at ~ 4 shots applied an HR mirror (λ = 1 064 nm, τ_{eff} = 3,5 ns, background pressure: 4 x 10^{-6} mbar; f_P 100 Hz)

5 Inspection techniques after the laser test sequence

5.1 General

Visual and microscopic inspection techniques are mandatory to examine the surface and the bulk of the optical component before and after the test according ISO 21254-1. For the identification of damaged sites on the tested specimen, an inspection of the surface is prescribed in ISO 21254-1 employing a Nomarski-type differential interference contrast microscope. However, other inspection methods can be used if they are proven to be in conformity with the prescribed interference contrast microscopy. In the following, examples for Nomarski microscopy and for alternative inspection methods will be described.

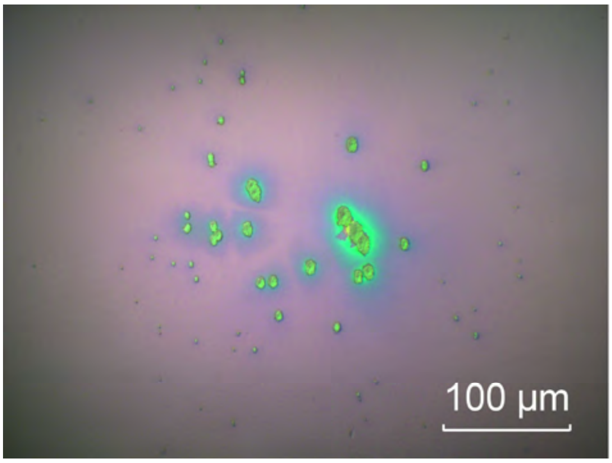

a) High reflecting mirror for Nd:YAG-Laser, E_0 = 78,2 J/cm², absorption-induced damage

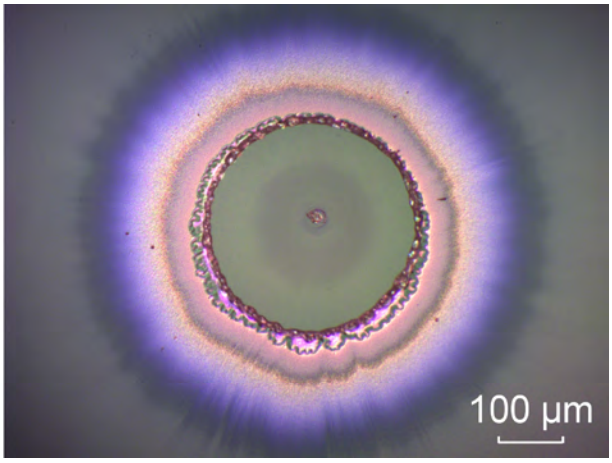

b) Antireflective coating for Nd:YAG-Laser, E_0 = 31,8 J/cm², defect-induced damage

Figure 12 — Illustration of Nomarski microscopic inspection techniques: Micrographs of different damage sites (test parameters: λ = 1 064 nm, τ_{eff} = 12 ns, d_{eff} = 298 µm)

5.2 Nomarski microscopy

Typical images taken with a Nomarski microscopic system, which is constructed according to the standard inspection technique described in ISO 21254-1, are displayed in Figure 12. For routine inspection and objective detection of laser damage, an image analyser may be attached to the microscope. For samples transparent in the visible spectral region, a visual inspection is recommended to locate the damage sites. If bulk damage is suspected, the focus of the microscope should be tuned through the volume of the optical component. Transmitting optical components not transparent in the visible spectral region (e.g. Ge, CdTe, Si) require investigation using cameras and microscopes adapted to the transparency range of the components.

5.3 Microscopic image comparator

The microstructure of laser radiation-induced damage on the surface or within a test piece is likely to be extremely complex. Whilst a scanning probe microscope would provide sufficient resolution it is considered impractical due to the test environment, the need for data reduction and cost. Optical methods are preferred provided they are objective with traceability. ISO 14997 describes an optical test method for surface imperfections and recommends the use of radiometric obscuration for imperfections with dimensions less than 10 µm. Larger damage centres can be measured with a travelling microscope. Opaque spots of known size are used in a substitution method in which the amount of radiation removed by a damage centre is equated to the amount of radiation removed by a spot of known size when both are illuminated and viewed under the same conditions. The damage is measured in micrometers called sed (spot-equivalent diameter) units.

A schematic representation of a simple low-cost microscope image comparator that can be used for quantifying damage, such as digs and scratches, is shown in Figure 13. Normal illumination is required due to the shape irregularity of damage that causes asymmetrical scatter patterns and a low aperture imaging system is employed to remove the optical effects of fine structure in the damage area. The instrument is based on a standard microscope with vertical illuminator 1,2,3 and spatial frequency filter 8, placed in the back focal plane of the microscope objective 7. A tungsten halogen lamp and condenser illuminates the pinhole source 1 that is at the focus of the collimator 2. The parallel beam produced is reflected downwards by the polarising beam splitter 3 to illuminate the test specimen 4.

The beam transmitted by 4 is returned by the retro-reflector 5 and two passages through the quarter wave plate 6. This plate is needed to allow the returned beam to be transmitted by 3 and imaged by 7 having passed through 8 and the high-aperture field lens 9. This is needed to converge the field rays down to be accepted by the small aperture lens in the camera 10. If 4 is a reflecting specimen 5 is removed as it is no longer required and 6 is placed between 3 and 4. Since even a quarter wavelength of defocus, resulting from an object movement of ~0,3 mm, can cause a change in value of the image contrast of ~20 % care is required in selecting the best focus. If available a visual image channel employing an eyepiece can be used for selecting the best 'peak' focus or alternatively the digital camera can be plugged into a TV. The LCD of the camera might not have sufficient resolution to perform this task with the necessary precision. With this instrument a damage centre appears, as a dark spot seen against a bright background. Having focused and operated the camera shutter the next task is to download the stored image into a PC supplied with image processing software. The image magnification on the screen should be adjusted to provide at least 10 pixels across the image to be measured. Image luminosity values are found from Image in the Menu Bar and then the digital display found in Histogram. The selection window of say 1x50 pixels is scanned manually across the image to determine the minimum luminosity value I_{min}. The maximum value I_{max} is obtained by displacing the selected window to one side of the image. The contrast C [%] is then calculated as $[I_{max} - I_{min}]/[I_{max} + I_{min}]\cdot 100$. Although a luminosity value can be quoted to 5 significant figures residual image clutter from background variations, errors in focal setting, residual polish defects and dust on components the uncertainty of detection of a high contrast feature is probably no better than ± 5 %. In order to convert the measured contrast of a damage centre image to a spot equivalent diameter (sed units) the instrument requires calibration using opaque spots of known dimensions. A graticule bearing opaque lines and spots according to the logarithmic series in the ISO standard is commercially available for this purpose. The lines are used for quantifying the severity of scratches in line-equivalent width or lew units.

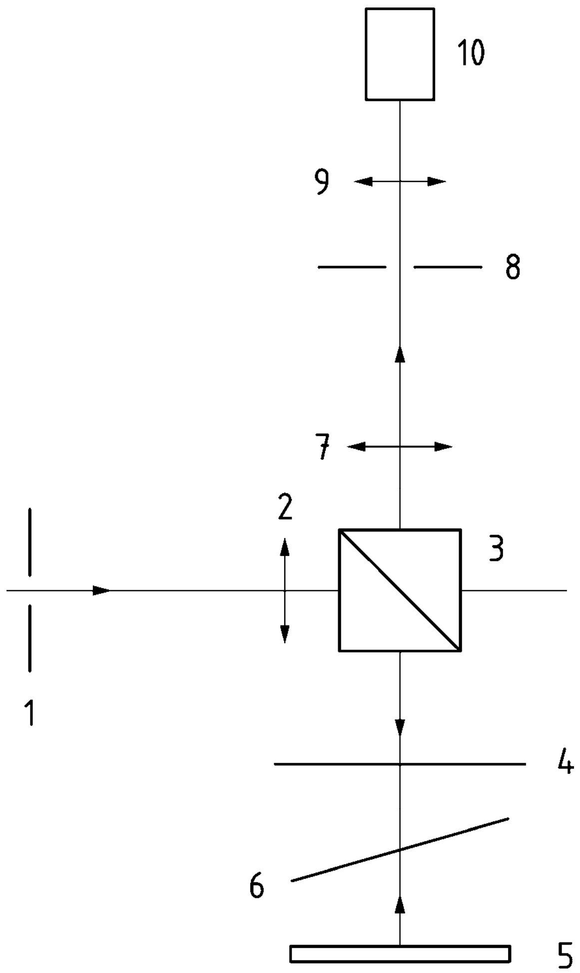

Key

1 pinhole
2 collimator
3 polarising beam splitter
4 specimen under test
5 retro-reflective screen
6 quarter-wave plate
7 imaging lens
8 pinhole
9 field lens
10 digital camera

Figure 13 — principle of a microscopic imaging comparator

5.4 Laser scanning microscopy

Laser scanning microscopes (LSM) are appropriate tools for a topographic inspection of single damage sites. In contrast to inspection techniques with electron microscopes, LSM can be performed on specimens of arbitrary size and surface figure. As a consequence of scanning in the plane and the depth, LSM offer the advantage of a direct recording of 3D-topographies of the area of interest on the sample (see Figure 14). LSM can be also adapted to a detection of the fluorescence intensity emitted by the sample area.

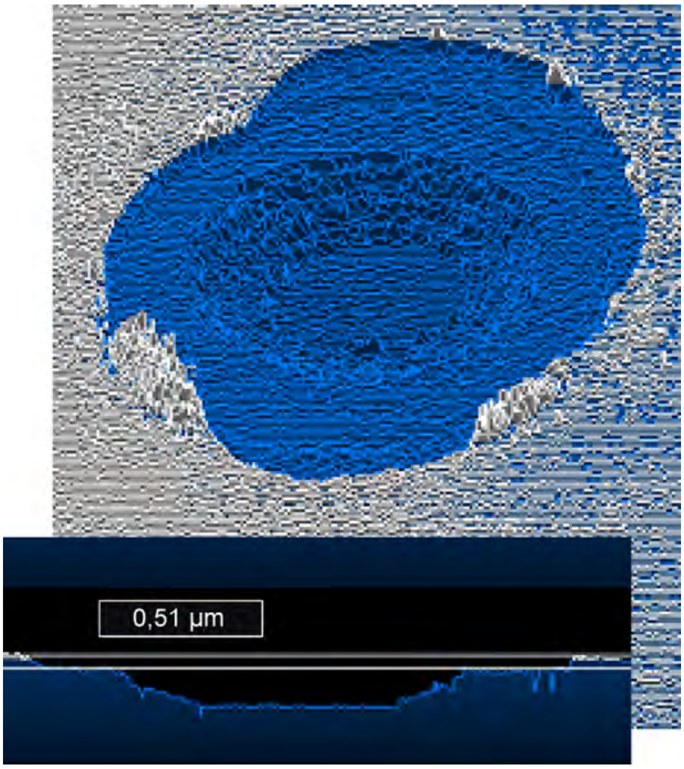

NOTE See Reference [12].

Figure 14 — Laser scanning micrograph (3D-topography) of a high reflecting mirror (IBS TiO_2/SiO_2) for ultra short pulse applications (Nd:YAG-Laser, τ_{eff} = 8 ns, d_{eff} = 184 µm)

5.5 Mapping techniques

For the identification of sites altered by laser radiation, different surface properties can be mapped. Besides scattering or absorptance, the reflectance or transmittance of the sample are quality parameters which can be influenced by laser irradiation. High precision detection devices for scanning of reflectance or transmittance at a single wavelength can be implemented on the basis of principles described in ISO 13697. For spectro-photometric analysis, mapping spectrophotometers can be employed (see Figure 15). Fast scanning devices with high sensitivity can be based on the detection of Total Scattering as described in ISO 13696.

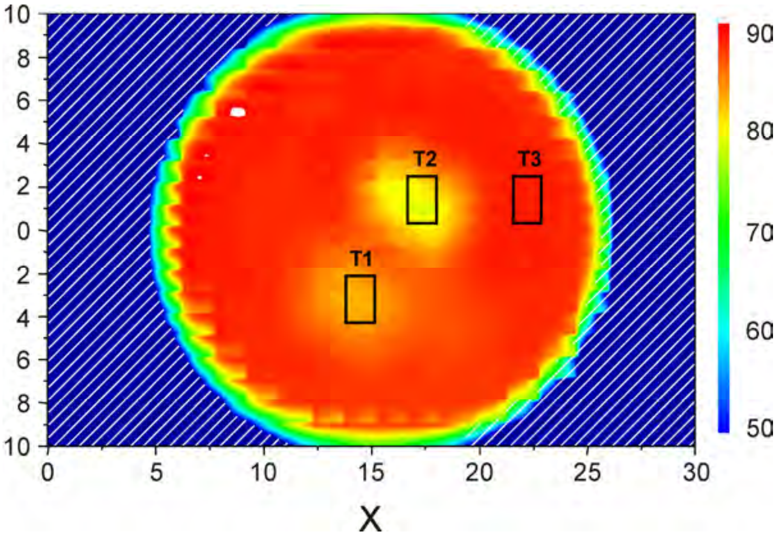

Key

X position [mm]

NOTE 1 The vertical axes show position [mm] (left) and transmittance [%] (right).

NOTE 2 See Reference [13].

Figure 15 — Spectrophotometric mapping of transmittance (λ = 193 nm, SiO_2-coating on quartz, optical thickness; 6 λ/4, spots; irradiated by 2 GeV synchrotron radiation)

5.6 Electron microscopy

Besides optical microscopy, inspection techniques with improved resolution on the basis of electron microscopy are suitable for damage inspection. Scanning electron microscopic (SEM) techniques allow for detailed investigations in the morphology of an individual damage site and can reveal additional information on the contributing damage mechanisms. The preparation of samples for SEM-techniques normally includes a fractioning of the specimen and an additional overcoating to improve the electrical conductivity of the surface. Typical SEM-micrographs of selected damage sites on dielectric optical coatings are depicted in Figure 16. As a consequence of the complex handling and preparation steps necessary for coating samples, the application of transmission electron microscopy is restricted to special investigations in the structure and morphology of damaged sites.

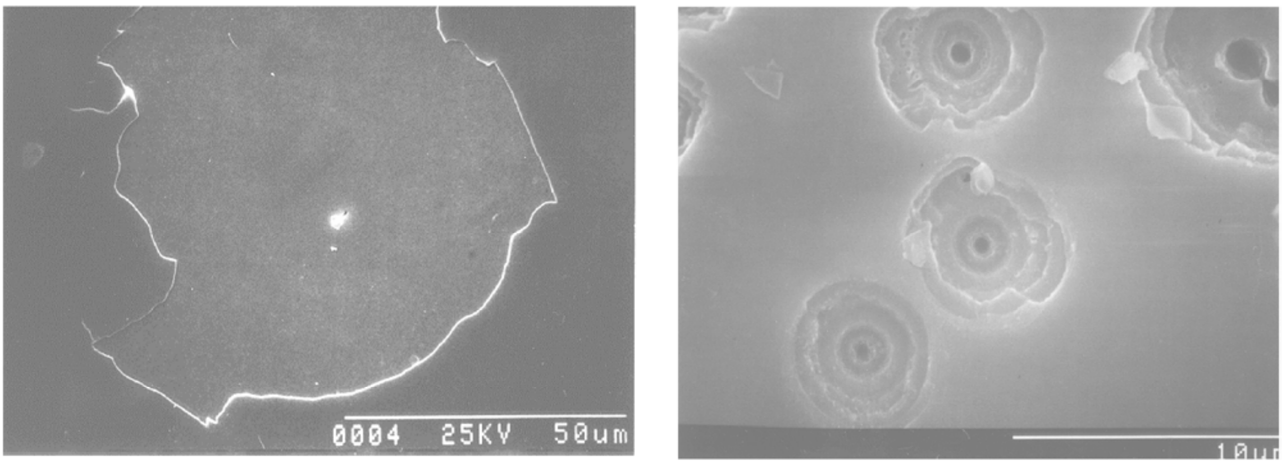

a) 2-QWOT-stack HfO_2/SiO_2, Nd:YAG-Laser, τ = 14 ns, E_0 = 45 J/cm², stress-induced damage, absorption-induced damage

b) QWOT-stack HfO_2/SiO_2, Nd:YAG-Laser, τ = 14 ns, defect-induced damage

Figure 16 — Illustration of electron microscopic inspection techniques: Micrographs of different damage sites

5.7 Atomic force microscopy

Due to its high lateral and vertical resolution of several nanometers, atomic force microscopy (AFM) can reveal the damage morphology in great detail as a true 3D surface profile, and can hence provide deep insights into the damage mechanism. Additionally, samples viewed by AFM do not require any special treatments (such as metal or carbon coatings) that would irreversibly change the sample properties. While an electron microscope needs a complex vacuum environment for proper operation, most AFM modules can work perfectly well in ambient air. Furthermore, compact AFM instruments are available in the meantime that can be operated as a part of an optical test bench. By removing the scanner head for laser irradiation of the sample and correct repositioning, the development of the laser damage morphology can be traced in an offline manner. An example is depicted in Figure 17, where morphology changes after consecutive shots applied to an AR coated window are shown.

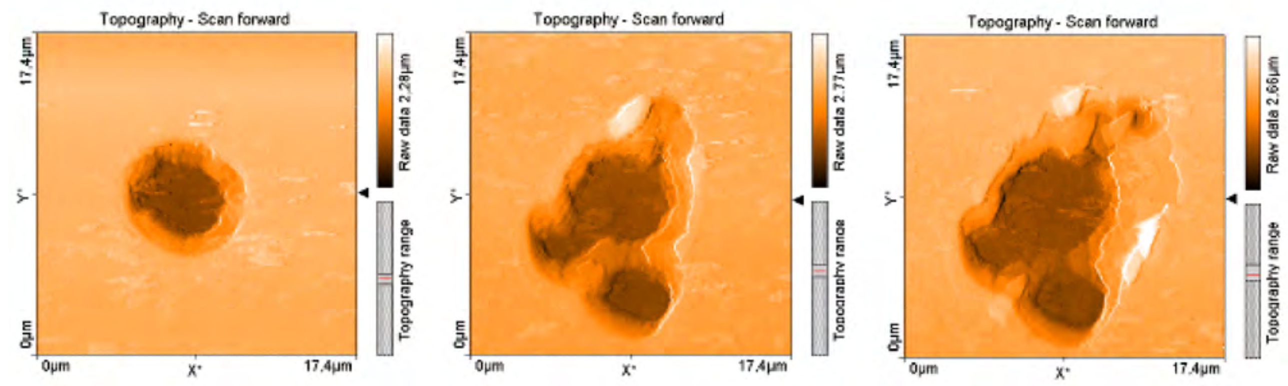

Figure 17 — AFM scans showing the development of laser damage after consecutive shots (1, 2 and 5 shots, left to right) applied to AR coated window (λ = 532 nm; fluence ~ 20 J/cm², τ = 3ns,d = 50 µm)

5.8 Confocal microscopy

Damage sites can be measured using a confocal microscope. A confocal microscope is an integrated microscope system consisting of a fluorescence microscope, laser light sources, a scan head which directs the laser radiation on the sample and collects the emission, a computer with software for controlling the scan head and displaying the acquired data. Confocal microscopes can be used in several modes, epi-fluorescence laser scanning mode (ELSM), reflectivity mode and transmitted mode. Excitation in ELSM induced by the laser point source arrives confocally on the sample. Fluorescent light emitted from the illuminated point is focused as a confocal point at the detector pinhole. Fluorescent light emitted from the out of focus point (above and below the focal plane) does not enter the pinhole and thus is not detected. By scanning the sample in x and y direction an image is reconstructed. To achieve a 3D reconstruction the x, y stage is motorized in z direction. For the separation of excitation and emitted light a dichroic mirror is used, and a filter is placed in front of the detector (Photomultiplier). In reflectivity laser scanning mode, the dichroic mirror is replaced by a partially reflecting mirror to direct the reflected light onto the photomultiplier. The reflected light is filtered by the pinhole to achieve the confocal resolution. The resolution values $\sigma_{x,y}$ in x and y directions, and σ_z in z direction in confocal microscopy are given by the following formulae

$$\sigma_{x,y} = 0{,}4\lambda / NA \tag{1}$$

$$\sigma_z = 1{,}4\lambda n / NA^2 \tag{2}$$

where NA is the numerical aperture, λ is the wavelength and n the optical index, respectively. Typical resolutions of approximately 150 nm in x-y direction and 300 nm in z direction are achieved depending on the objectives used.

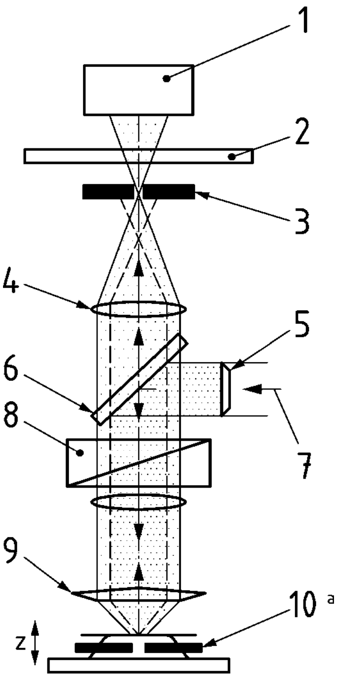

a) Confocal microscopy principle; epifluorescence mode (see Reference [14])

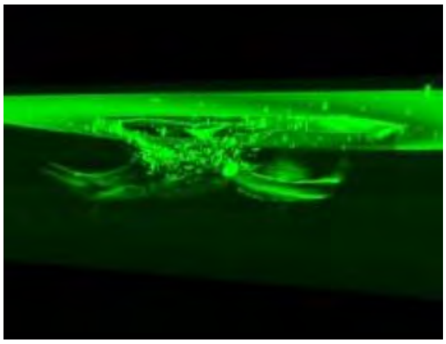

b) Typical morphology of a damage site observed with confocal microscopy (3D picture)

Key

1 photomultiplier

2 emission filter

3 pinhole

4 lens

5 expander

6 dichroir mirror

7 laser beam

8 scanner

9 objective lens

10 focal plane

a Focal plane varies in z direction.

Figure 18 — Principle of confocal microscopy

A typical morphology of a damage site revealed on the rear face of a fused silica component is reported (see Figure 18) as example of confocal microscope characterization: it represents not only what is on the surface but also the cracks under the surface.

Bibliography

[1] ISO 10110-7, *Optics and photonics — Preparation of drawings for optical elements and systems — Part 7: Surface imperfection tolerances*

[2] ISO 13696, *Optics and optical instruments — Test methods for radiation scattered by optical components*

[3] ISO 13697, *Optics and photonics — Lasers and laser-related equipment — Test methods for specular reflectance and regular transmittance of optical laser components*

[4] ISO 14997, *Optics and photonics — Lasers and laser-related equipment — Test methods for surface imperfections of optical elements*

[5] K. STARKE, T. GROß and D. RISTAU, *Laser-induced damage investigation in chirped mirrors for ultrashort pulse laser systems*, in Proc. of SPIE, vol. 4347 (edited by G.J. Exarhos, A.H. Guenther, M.R. Kozlowski, K.L. Lewis and M.J. Soileau), pp. 528–534, Proceedings of the 32th Annual Symposium on Laser-Induced Damage in Optical Materials, 2001

[6] H. KÜSTER and J. EBERT, *Pyroelectric measurement of absorption in oxide layers and correlation to damage threshold.*, in NBS Special Publication vol. 568 (edited by H.E. Bennett, A.J. Glass, A.H. Guenther and B.E. Newnam), pp. 269-281, Proceedings of the 10th Annual Symposium on Laser-Induced Damage in Optical Materials, 1979

[7] K. STARKE, T. GROß, D. RISTAU, W. RIGGERS and J. EBERT, *Laser-induced damage threshold of optical components for high repetition rate Nd:YAG-lasers*, in Proc. of SPIE, vol. 3578 (edited by H.E. Bennett, A.H. Guenther, M.R. Kozlowski, B.E. Newnam and M.J. Soileau), pp. 584–593, Proceedings of the 30th Annual Symposium on Laser Induced Damage in Optical Materials, 1999

[8] W. PLAß and A. GIESEN, *Stress- and defect damage of CO2-laseroptics: time of damage analysis*, in Proc. of SPIE, vol. 2714 (edited by H.E. Bennett, A.H. Guenther, M.R. Kozlowski, B.E. Newnam and M.J. Soileau), pp. 166–176, Proceedings of the 27th Annual Symposium on Laser-Induced Damage in Optical Materials, 1995

[9] M. RAHE, E. OERTEL, L. REINHARDT, D. RISTAU and H. WELLING, *Absorption Calorimetry and Laser Induced Damage Threshold Measurements of AR-coated ZnSe and Metal Mirrors at 10.6 µm*, Proc. Of SPIE (edited by H.E. Bennett, L.L. Chase, A.A. Guenther, B.E. Newnam and M.J. Soileau), vol. 1441, pp. 113-126, Proceedings of the 22nd Annual Symposium on Laser-Induced Damage in Optical Materials, 1990

[10] H. BLASCHKE, D. RISTAU, E. WELSCH and O. APEL, *Absolute Measurements of non-linear Absorption near LIDT at 193 nm*, in Proc. of SPIE, vol. 4347 (edited by G.J. Exarhos, A.H. Guenther, M.R. Kozlowski, K.L. Lewis and M.J. Soileau), pp. 447–453, Proceedings of the 32th Annual Symposium of Laser Induced Damage in Optical Materials, 2001

[11] L. BAKER, *Surface damage metrology: precision at low cost*, in Proc. of SPIE Vol. 4779 (edited by. A. Duparré and B. Singh) pp. 41-51, Proceedings of Advanced Characterization Techniques for Optical, Semiconductor, and Data Storage Components, 2002

[12] B. WU, U. BARTUCH, M. JUPÉ, L. JENSEN, M. LAPPSCHIES, K. STARKE and D. RISTAU, *Morphology investigations of laser induced damage*, in Proc. of SPIE, vol. 6403 (edited by G.J. Exarhos, A.H. Guenther, K.L. Lewis, D. Ristau, M.J. Soileau and C.J. Stolz), p. 640319 ff., Proceedings of the 38th Annual Symposium on Optical Materials for High Power Lasers, 2006

[13] S. GÜNSTER, H. BLASCHKE, K. STARKE, D. RISTAU, M. DANAILOV, B. DIVIACCO, A. GATTO, N. KAISER, F. SARTO, and E. MASETTI, *Surface investigation of VUV-optical components after exposure to high energetic synchrotron radiation*, in Proc. of SPIE, vol. 5273 (edited by G.V. Klimusheva, A.G. Iljin and S.A. Kostyukevych), pp. 281-287, Proceedings of the Ninth International Conference on Nonlinear Optics of Liquid and Photorefractive Crystals, 2004

[14] J. NEAUPORT, P. CORMONT, P. LEGROS, C. AMBARD and J. DESTRIBATS, *Imaging subsurface damage of grinded fused silica optics by confocal fluorescence microscopy*, Opt. Express **17**, 3543-3554, 2009

[15] L. LAMAIGNÈRE, V. CAVARRO, C. ALLAIS, D. BERNARDINO, M. JOSSE and H. BERCEGOL, *Time-resolved measurements of reflectivity, plasma formation and damage of Hafnia/Silica multilayers mirrors at 1064 nm*, in Proc. of SPIE, vol. 4679 (edited by G.J. Exarhos, A.H. Guenther, M.R. Kozlowski, K.L. Lewis and M.J. Soileau), pp. 410-419, Proceedings of the 33th Annual Symposium on Laser-Induced Damage in Optical Materials, 2001

[16] A. DURING, M. COMMANDRÉ, C. FOSSATI, B. BERTUSSI, J.Y. NATOLI, J.L. RULLIER and P. BOUCHUT, *Integrated photothermal microscope and laser damage test facility for in-situ investigation of nanodefect induced damage*, Optics express 11, 2497 (2003)

[17] A. DURING, C. FOSSATI and M. COMMANDRÉ, *Photothermal deflection microscopy for imaging sub-micronic defects in optical materials*, Optics Communications **230**, 279 (2004)

[18] B. BERTUSSI, J.Y. NATOLI and M. COMMANDRÉ, *High resolution photothermal microscope: a very sensitive tool for the detection of isolating absorbing defects in optical coatings*, Applied optics **45**, 1410 (2006)

ICS 31.260

Price based on 20 pages